

New Route to Synthesize Highly Active Nanocrystalline Sulfated Titania–Silica: Synergetic Effects between Sulfate Species and Silica in Enhancing the Photocatalysis Efficiency

Chao Xie, Qiuqing Yang,* Zili Xu, Xingjuan Liu, and Yaoguo Du

College of Environment and Resources, Jilin University, Changchun 130023, China

Received: January 13, 2006; In Final Form: March 11, 2006

A simple and efficient approach has been set up for fabricating highly active sulfated titania–silica ($\text{SO}_4^{2-}/\text{TiO}_2\text{--SiO}_2$): $\text{Ti}(\text{SO}_4)_2$ was hydrolyzed in the presence of silica, making it possible to sulfate titania and form titania–silica mixed oxide in one step. This study was focused on investigating the roles of sulfate species and silica in improving the physicochemical properties and photoactivity of $\text{SO}_4^{2-}/\text{TiO}_2\text{--SiO}_2$ through comparison with sulfated titania ($\text{SO}_4^{2-}/\text{TiO}_2$) and sulfate-free catalysts (TiO_2 and $\text{TiO}_2\text{--SiO}_2$). Various characterization methods, including X-ray diffraction (XRD), Fourier transform infrared spectroscopy (FT-IR), X-ray photoelectron spectroscopy (XPS), and surface photovoltage spectroscopy (SPS), were employed to test these materials. The results revealed that for $\text{SO}_4^{2-}/\text{TiO}_2$ and $\text{TiO}_2\text{--SiO}_2$ the sole presence of either sulfate species or silica imposes negative effects on the photocatalysis behavior of titania, leading them to have negligible photoactivities. On the contrary, in the case of $\text{SO}_4^{2-}/\text{TiO}_2\text{--SiO}_2$, sulfate species and silica were proved to act in a cooperative manner; therefore, the following enhanced structure and surface properties of $\text{SO}_4^{2-}/\text{TiO}_2\text{--SiO}_2$ were obtained: (i) relatively well-crystallized and smaller-size (15.4 nm) anatase-phase titania was formed upon 500 °C calcination without forming rutile phase and (ii) the formation of active surface sulfate species promotes the separation of photoinduced electron–hole pairs and therefore accelerates the photocatalysis reaction. Therefore, its photoactivity is enhanced as a result of the favorable synergetic effects between sulfate species and silica due to their simultaneous presence.

Introduction

In past decades extensive research has focused on nanosized materials, motivated by the remarkable demands of various technological applications, such as water splitting and photocatalysis.^{1–4} Among these materials titania is of particular interest as a semiconductor photocatalyst because illumination of titania with light possessing greater energies than its band-gap energy can trigger electron transitions from the valence band to the conduction band, leaving positive holes behind. The photocatalysis behavior is initiated by the surface trapping of photoinduced electron–hole pairs, inducing interfacial charge-transfer reactions with the target pollutant molecules, resulting in their complete degradation to CO_2 .^{1,2}

Although photodegradation of various pollutants over titania is considered as a powerful technique for treating contaminated air and water discharges, it faces several significant limitations. The major constraint is its lower efficiency due to the rapid recombination of photoinduced electron–hole pairs. For circumventing many of these problems a number of strategies including surface photosensitizing, noble metal deposition, and modification with other composites, as well as doping of metal and nonmetal ions, have been proposed.^{1,2} In particular, sulfation of semiconductor photocatalysts is of great interest for scientists and engineers because they have an enormous potential for environmental pollutant remediation.^{5–7} For instance, Ward and Ko prepared sulfated zirconia and systematically studied the effects of changing the sulfur content and activation temperature on the variations of its surface and structure properties.⁷ They classified surface sulfate species into two forms: active surface

sulfate species containing covalent S=O bonds with a strong electron-withdrawing effect and inactive surface sulfate species possessing more ionic character in nature with weak electron induction potential. They believed the prerequisite of activating sulfate species is to form a regular crystal structure that might help charge transfer and delocalization in the vicinity of sulfate species. However, some obvious drawbacks of the traditional impregnation method for preparing sulfated catalysts limit its wide applications;^{5–7} e.g., to anchor sulfate species onto the surface catalysts with large surface area and porous structure are preferred, needing various expensive and complicated techniques, such as supercritical drying.⁷ Thus, we believe developing a simple and efficient approach to produce sulfated catalysts should be meaningful work.

Titania–silica mixed oxide is also a class of promising materials in the field of environmental pollutant remediation because mixing titania with a suitable amount of silica can not only utilize its photocatalysis capability, but also greatly improve its thermal stability.^{8–13} The high efficiency of titania–silica mixed oxide should be predominately attributed to the intimate molecule-level interaction between titania and silica, which may lead to many new physicochemical properties, such as quantum-sized crystallites, high surface area, and high adsorption capability toward the pollutants.^{9–13}

We can see that either sulfation of titania or mixing titania with silica may be an effective way to enhance the photoactivity of titania. One can imagine that if these two methods are combined together to synthesize sulfated titania–silica, higher photocatalysis efficiency should be readily achieved because this catalyst may take advantage of both sulfate species and silica. To our knowledge, very little research has focused on

* Corresponding author. E-mail: yangqj@email.jlu.edu.cn.

this aspect, and it is most common to synthesize sulfated titania–silica via the traditional method: formation of titania–silica sol by hydrolyzing the corresponding metal alkoxide and development of a three-dimensional gel network of titania–silica hydroxide, followed by the sulfation process.^{14–16}

Driven by the need of overcoming the limitations of the titania photocatalysis technique and seeking an alternative method to produce sulfated titania–silica, a simple and efficient approach was explored. In this study, we present the synthesis, characterization, and photoactivity behavior of sulfated/sulfate-free photocatalysts. Our objective is to interpret the enhancement of physicochemical properties and photocatalysis efficiency of $\text{SO}_4^{2-}/\text{TiO}_2\text{--SiO}_2$ in terms of the favorable synergetic effects between sulfate species and silica due to their simultaneous presence.

2. Experimental Section

2.1. Preparation of Catalysts. All chemicals in this study were used as received without any further purification. For preparing $\text{SO}_4^{2-}/\text{TiO}_2\text{--SiO}_2$, 2.25 mL of tetraethyl orthosilicate (TEOS, 98%) was mixed with 10.8 mL of double-distilled water, 23.9 mL of ammonium hydroxide (NH_3 , 28%), and 2 mL of anhydrous ethanol, and then this solution was dried under an infrared lamp. Subsequently, the silica as-obtained was added into 50 mL of 1 M $\text{Ti}(\text{SO}_4)_2$. Finally 23.9 mL of ammonium hydroxide (NH_3 , 28%) was added dropwise into the above solution under vigorous stirring to form hydroxide. $\text{SO}_4^{2-}/\text{TiO}_2$ was prepared by an identical procedure, merely without adding silica. For preparing sulfate-free catalysts (TiO_2 and $\text{TiO}_2\text{--SiO}_2$), BaCl_2 solution was slowly added into $\text{Ti}(\text{SO}_4)_2$ solution to remove SO_4^{2-} ions. After BaSO_4 precipitates were separated from the supernatant, the subsequent procedures were the same as those of $\text{SO}_4^{2-}/\text{TiO}_2$ and $\text{SO}_4^{2-}/\text{TiO}_2\text{--SiO}_2$. Finally, the resultant hydroxides were centrifuged and washed by double-distilled water until the supernatant liquid was neutral and free of Cl ions (negative AgNO_3 test). To further remove the residual SO_4^{2-} ions, the hydroxides were put into a dialysis bag (Union Carbide Corp.) that was in a beaker filled with double-distilled water under vigorous stirring until no SO_4^{2-} ions were detected from the double-distilled water. Finally, all samples were calcined at 500 °C for 2 h in air.

2.2. Catalyst Characterization. The crystalline phase was characterized by a Bruker D8 GADDS X-ray diffractometer using Cu K α radiation ($\lambda = 1.54056$ Å). In addition, the crystalline size D was estimated from the width of lines in the X-ray pattern with the aid of the Scherrer formula: $D = 0.9 \lambda / (\beta \cos \theta)$, where λ is the wavelength of the X-ray used and β is the width of the line at the half-maximum intensity. FT-IR spectra on pellets of the samples mixed with KBr were obtained utilizing a Nicolet Impact 410 Fourier transform infrared spectrophotometer at a resolution of 4 cm^{-1} . X-ray photoelectron spectroscopy (XPS) measurements were performed in a VG ESCALAB MKII X-ray photoelectron spectrometer. The X-ray source emitted Mg K α radiation (1253.6 eV). For all the binding energy obtained the pressure was maintained at 6.3×10^{-7} Pa. Binding energies were calibrated with respect to the signal for adventitious carbon (binding energy = 284.6 eV). Quantitative analysis was carried out using the sensitivity factors supplied with the instrument. Surface photovoltage spectroscopy (SPS) were obtained with the surface photovoltage spectrometer that has been described elsewhere.¹⁷

2.3. Photocatalytic Reaction System. The photoactivity tests for degrading heptane were carried out at ambient temperature using a 300 mL cylindrical quartz tube (4.4 cm i.d. and 20 cm

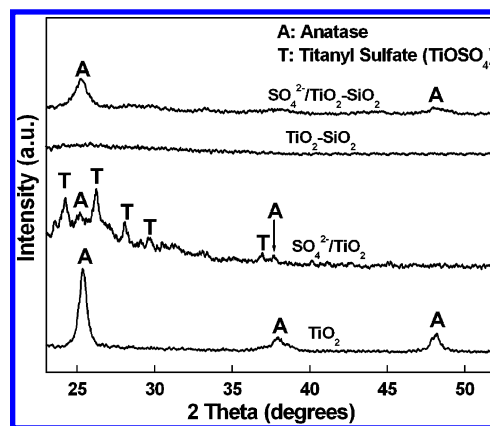


Figure 1. XRD patterns of the catalysts.

length). In the experiment 0.1 g of catalyst was spread uniformly over the bottom surface of the reactor in the form of powders. After this the reactor was evacuated and filled with heptane (0.1%, v/v), oxygen (20%, v/v), and balance nitrogen to a total pressure of 1 atm. The reaction was started by turning on a 400 W high-pressure mercury lamp. Subsequently, the concentration of reactant in the reactor was monitored by a Hewlett-Packard 4890D gas chromatograph equipped with a flame ionization detector (FID). The yield of CO_2 was determined by GC equipped with a thermal conductivity detector (TCD) and a Porapak QS stainless steel column.

The photoactivities of the catalysts were quantitatively evaluated by calculating the apparent reaction rate constants according to the equation¹⁸ $\ln(C_0/C) = k_a t$, where C_0 is the initial concentration of heptane in the reactor after dark adsorption, C is the concentration of heptane at reaction time t , and k_a is the apparent pseudo-first-order rate constant. According to this equation a graph can be drawn by plotting $\ln(C_0/C)$ vs reaction time t ; then the slope equal to k_a can be obtained. The mineralization degree was calculated by C_1/C_2 , where C_1 is the concentration of produced CO_2 at $t = 30$ min and C_2 is the amount of CO_2 if all heptane is degraded into CO_2 .

3. Results and Discussion

3.1. XRD Study. Figure 1 gives the XRD patterns of the catalysts. Apparently, upon calcination TiO_2 shows strong (101), (004), and (200) anatase diffraction peaks at 25.2°, 37.8°, and 48.0°. However, in the case of $\text{SO}_4^{2-}/\text{TiO}_2$, only two weak anatase diffraction peaks around 25.2° and 37.8° are observed. Interestingly, we can see that the diffraction peaks attributed to titanyl sulfate (TiOSO_4)¹⁹ are much stronger than the anatase diffraction peaks. Therefore, XRD results suggest that the presence of sulfate species is capable of inhibiting the crystallization of titania due to the generation of sulfate–titania complexes, which can suppress formation of regular Ti–O networks.

In the previous study it was well established that for titania–silica mixed oxide the crystallization of titania may be retarded by forming Ti–O–Si linkages.^{9–13} At the interface of titania and silica SiO_2 lattices lock Ti–O species and prevent the nucleation of titania, which is the exact reason $\text{TiO}_2\text{--SiO}_2$ is amorphous. In terms of XRD results of $\text{SO}_4^{2-}/\text{TiO}_2$ and $\text{TiO}_2\text{--SiO}_2$, both confirming the presence of either sulfate species or silica is effective in prohibiting the crystallization of titania, it is reasonable to deduce that the crystallization of $\text{SO}_4^{2-}/\text{TiO}_2\text{--SiO}_2$ should be further suppressed in the simultaneous presence of sulfate species and silica. However, it is interesting to note that $\text{SO}_4^{2-}/\text{TiO}_2\text{--SiO}_2$ exhibits evident anatase diffraction peaks

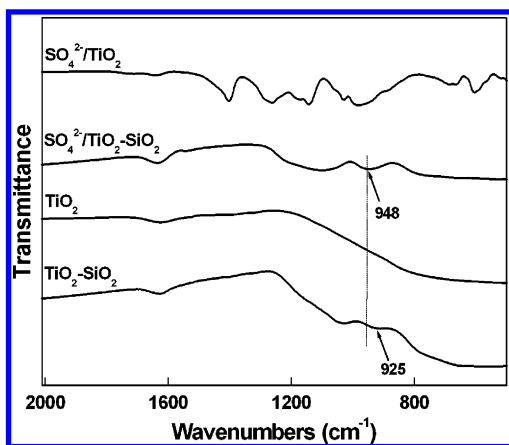


Figure 2. FT-IR spectra of the catalysts in the range of 2000–500 cm^{-1} .

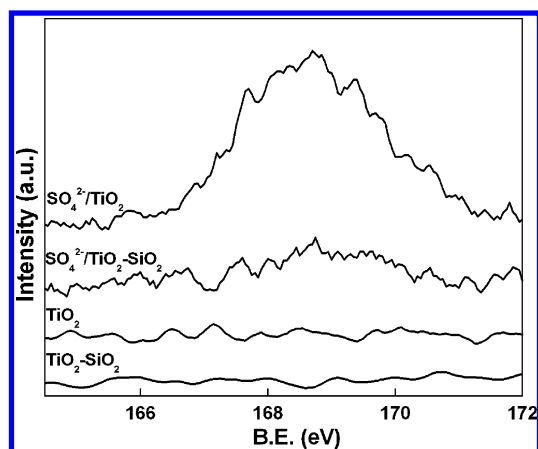


Figure 3. XPS spectra of S 2p for the catalysts.

without forming titanyl sulfate. This fact discloses an interesting phenomenon: although either sulfate species or silica can substantially prohibit the crystallization of titania, the simultaneous presence of sulfate species and silica may no longer inhibit the crystallization like $\text{SO}_4^{2-}/\text{TiO}_2$ and $\text{TiO}_2\text{-SiO}_2$.

3.2. FT-IR Study. FT-IR spectra in the range of 2000–500 cm^{-1} are shown in Figure 2. Several useful pieces of information can be found: (i) for $\text{SO}_4^{2-}/\text{TiO}_2\text{-SiO}_2$, the band around 948 cm^{-1} can be assigned to Ti–O–Si linkages, revealing the formation of an intimate molecule-level interaction between titania and silica.²⁰ It is worth noting that the IR band of the Ti–O–Si linkages in $\text{TiO}_2\text{-SiO}_2$ is located at 925 cm^{-1} , obviously lower than that of $\text{SO}_4^{2-}/\text{TiO}_2\text{-SiO}_2$. This implies that the presence of sulfate species influences the interaction between titania and silica. (ii) For $\text{SO}_4^{2-}/\text{TiO}_2\text{-SiO}_2$ the broad band between 1250 and 1100 cm^{-1} reveals that the structure of sulfate species in this sample is of inorganic chelating bidentate containing strongly covalent S=O bonds.^{7,21,22} Such a structure has a strong electron-withdrawing effect on the neighboring Ti species, which is believed to be a strong driving force to modify the surface properties of titania. By contrast, $\text{SO}_4^{2-}/\text{TiO}_2$ has entirely different FT-IR bands as compared with $\text{SO}_4^{2-}/\text{TiO}_2\text{-SiO}_2$, indicating that addition of silica alters the binding manner of sulfate species with titania.

3.3. XPS Analysis. To identify the alteration of surface properties with the addition of silica, XPS measurements were carried out to calibrate the binding energy (B.E.) of S 2p, Ti 2p, and O 1s as well as Si 2p. As shown in Figure 3, $\text{SO}_4^{2-}/\text{TiO}_2$ has a much stronger XPS peak assigned to surface sulfate species due to formation of inert titanyl sulfate. As silica is

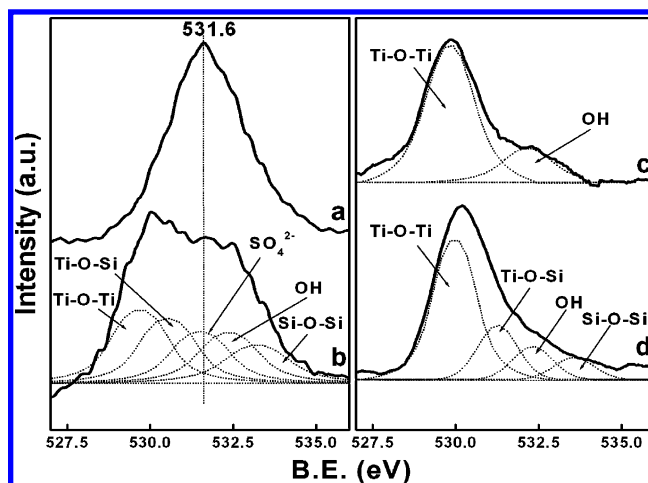


Figure 4. XPS spectra of the O 1s region for the catalysts: (a) $\text{SO}_4^{2-}/\text{TiO}_2$, (b) $\text{SO}_4^{2-}/\text{TiO}_2\text{-SiO}_2$, (c) TiO_2 , and (d) $\text{TiO}_2\text{-SiO}_2$.

TABLE 1. Physicochemical Properties of the Catalysts

catalysts	crystalline size (nm)	content of S element (at. %)
$\text{SO}_4^{2-}/\text{TiO}_2$		19.1
TiO_2	32.8	
$\text{SO}_4^{2-}/\text{TiO}_2\text{-SiO}_2$	15.4	3.3
$\text{TiO}_2\text{-SiO}_2$		

introduced the peak intensity of surface sulfate species is sharply decreased, and the XPS results reveal sulfur content is reduced from 19.1 at. % in $\text{SO}_4^{2-}/\text{TiO}_2$ to 3.3 at. % in $\text{SO}_4^{2-}/\text{TiO}_2\text{-SiO}_2$ (Table 1). Additionally, it is worth mentioning that no XPS peak associated with sulfate species can be detected in TiO_2 and $\text{TiO}_2\text{-SiO}_2$ as well as the absence of FT-IR bands of sulfate species in these two catalysts (Figure 2), reflecting that SO_4^{2-} ions were effectively removed for sulfate-free catalysts.

XPS spectra of the O 1s region are given in Figure 4. It is obvious that the O 1s region of TiO_2 can be resolved into lattice oxygen (Ti–O–Ti) and surface hydroxyl groups (Ti–OH), while that of $\text{TiO}_2\text{-SiO}_2$ contains lattice oxygen (Ti–O–Ti, Ti–O–Si, and Si–O–Si) and Ti–OH.²⁰ As for $\text{SO}_4^{2-}/\text{TiO}_2$, it shows a symmetrical peak centered at 531.6 eV that is the characteristic XPS peak of oxygen in surface sulfate species, revealing that its surface is predominantly covered by sulfate species. However, with the introduction of silica, the O 1s region of $\text{SO}_4^{2-}/\text{TiO}_2\text{-SiO}_2$ is significantly changed, and curve fitting suggests lattice oxygen (Ti–O–Ti, Ti–O–Si, and Si–O–Si), oxygen in surface sulfate species (SO_4^{2-}), and Ti–OH exist.^{4,20}

Figure 5 shows the Ti 2p_{3/2} B.E. value of $\text{SO}_4^{2-}/\text{TiO}_2$ is located at 459.4 eV, much higher than that of $\text{SO}_4^{2-}/\text{TiO}_2\text{-SiO}_2$ due to the strong electron-withdrawing effect of surface sulfate species.⁷ The Ti 2p_{3/2} peak of $\text{SO}_4^{2-}/\text{TiO}_2\text{-SiO}_2$ can be broken into two parts, one at 458.4 eV corresponding to Ti^{4+} species and another at 459.4 eV resulting from the titania combining with the surface sulfate species. These obvious distinctions between $\text{SO}_4^{2-}/\text{TiO}_2$ and $\text{SO}_4^{2-}/\text{TiO}_2\text{-SiO}_2$ demonstrate that the addition of silica facilitates removal of sulfate species, thus allowing titania to take part in photocatalysis reactions.

Figure 6 displays the XPS spectra of Si 2p for $\text{TiO}_2\text{-SiO}_2$ and $\text{SO}_4^{2-}/\text{TiO}_2\text{-SiO}_2$. Si 2p spectra of these two samples can be divided into two peaks at 102.1 and 103.6 eV, which can be attributed to silica in Ti–O–Si and Si–O–Si linkages, respectively.²³ It should be noted that for $\text{SO}_4^{2-}/\text{TiO}_2\text{-SiO}_2$, due to the surface sulfate species that can exist between titania

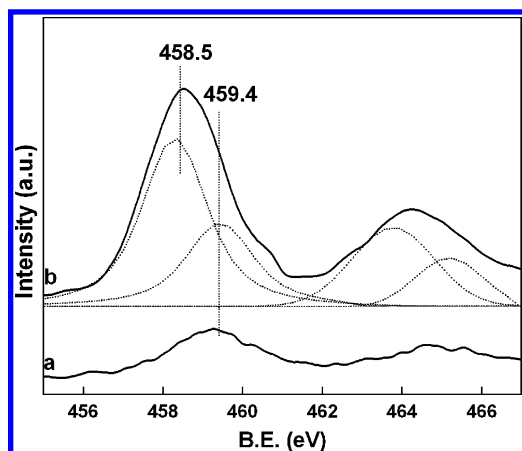


Figure 5. XPS spectra of Ti 2p for (a) $\text{SO}_4^{2-}/\text{TiO}_2$ and (b) $\text{SO}_4^{2-}/\text{TiO}_2\text{-SiO}_2$.

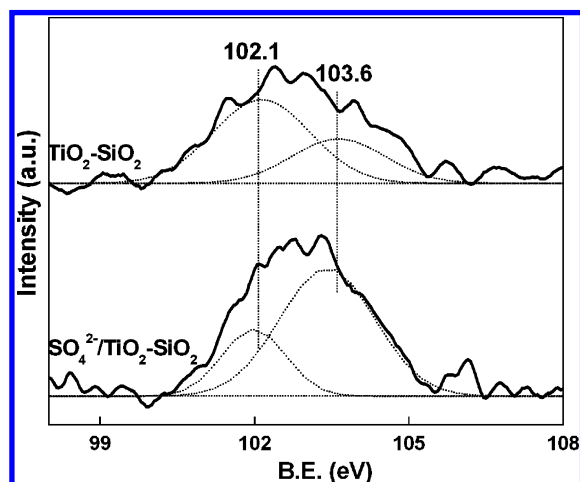


Figure 6. XPS spectra of Si 2p for the catalysts.

and silica as a protection layer to hinder interaction between them, silica mainly exists in Si—O—Si linkages, inducing the intensity of Si—O—Si linkages to be greater than that of Ti—O—Si. However, in $\text{TiO}_2\text{-SiO}_2$ the intensity of Ti—O—Si linkages is obviously greater than that of Si—O—Si linkages, illustrating that silica in $\text{TiO}_2\text{-SiO}_2$ predominately exists as Ti—O—Si linkages because silica may have more opportunities to interact with titania in the absence of sulfate species. Hence, we believe this difference of the interaction between titania and silica in the presence or absence of surface sulfate species is the reason the IR band of Ti—O—Si linkages in $\text{TiO}_2\text{-SiO}_2$ is located at 925 cm^{-1} while that of $\text{SO}_4^{2-}/\text{TiO}_2\text{-SiO}_2$ is at 948 cm^{-1} .

The XRD, FT-IR, and XPS results reveal that in the case of $\text{SO}_4^{2-}/\text{TiO}_2\text{-SiO}_2$ the presence of surface sulfate species alters the interaction between titania and silica; on the other hand, introduction of silica facilitates the decomposition of sulfate species, which can be interpreted by the fact that the sulfate species on silica is not stable and will be significantly decomposed beyond $250\text{ }^\circ\text{C}$.¹⁴ For $\text{SO}_4^{2-}/\text{TiO}_2$ sulfate species combine with titania to form inert titanyl sulfate that is thermally stable up to $600\text{ }^\circ\text{C}$. As a result, upon $500\text{ }^\circ\text{C}$ calcination a large amount of sulfate species will be retained on $\text{SO}_4^{2-}/\text{TiO}_2$, as shown in Figure 7A. With respect to $\text{SO}_4^{2-}/\text{TiO}_2\text{-SiO}_2$, part of the sulfate species will be deposited on silica and decomposed upon calcination (Figure 7B). Therefore, the amount of sulfate species in the catalyst is reduced, allowing titania to be crystallized into the anatase phase with exposed surfaces that can take part in photocatalysis reactions. We infer that, in our

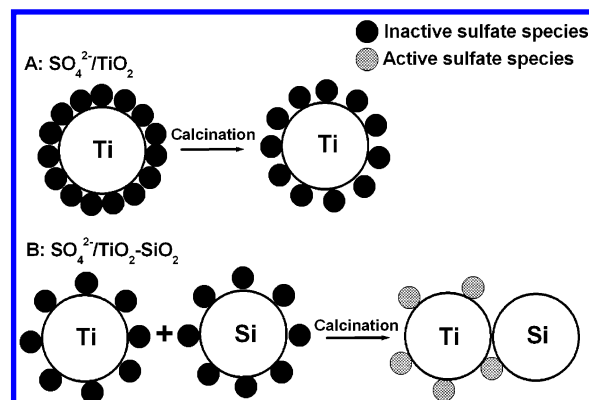


Figure 7. Schematic diagram of the variations of physicochemical properties with addition of silica.

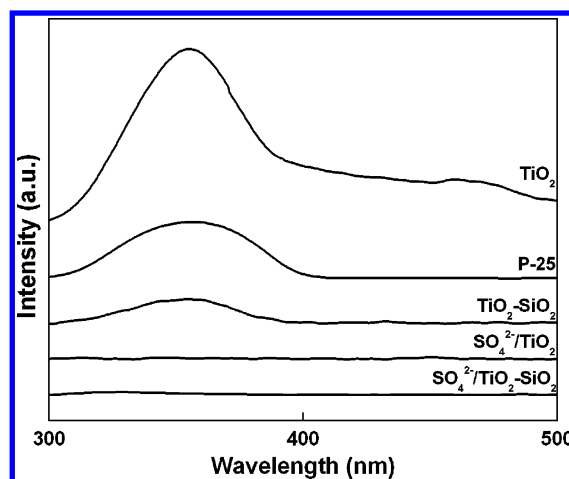


Figure 8. SPS spectra of the catalysts.

study, the sole presence of either sulfate species or silica imposes negative effects on the resultant catalysts ($\text{SO}_4^{2-}/\text{TiO}_2$ and $\text{TiO}_2\text{-SiO}_2$). However, the structure and surface properties of $\text{SO}_4^{2-}/\text{TiO}_2\text{-SiO}_2$ are significantly enhanced because the simultaneous presence of sulfate species and silica can produce the favorable synergetic effects: (i) silica is able to promote the decomposition of sulfate species and avoid the formation of inert titanyl sulfate and (ii) sulfate species existing between titania and silica act as a protection layer to hinder their excessive interaction, allowing $\text{SO}_4^{2-}/\text{TiO}_2\text{-SiO}_2$ to crystallize into the anatase phase without forming the rutile phase upon $500\text{ }^\circ\text{C}$ calcination.

3.4. SPS Measurements. To clarify the impact of sulfate species and silica on the separation and transportation of photoinduced charge carriers, surface photovoltage spectroscopy (SPS) was employed to characterize the catalysts because it can provide important information about the surface, interface, and bulk properties of semiconductor photocatalyst.²⁴ Figure 8 shows SPS spectra of the catalysts as well as that of P-25 for comparison. We can see with the removal of SO_4^{2-} ions, which can act as the traps to capture the photoinduced charges, TiO_2 possesses a much stronger SPS signal, evidencing its high recombination rate of photoinduced electrons and holes.²⁴ Note that the SPS intensity of $\text{TiO}_2\text{-SiO}_2$ is obviously lower in comparison with TiO_2 . This can be interpreted by its amorphous feature, which means a larger number of photoinduced electrons and holes will be consumed by the bulk defects that provide the sites for the recombination of photocarriers so that they cannot reach the surface. It is normal that $\text{SO}_4^{2-}/\text{TiO}_2$ does not exhibit a SPS signal in that its surface is predominantly

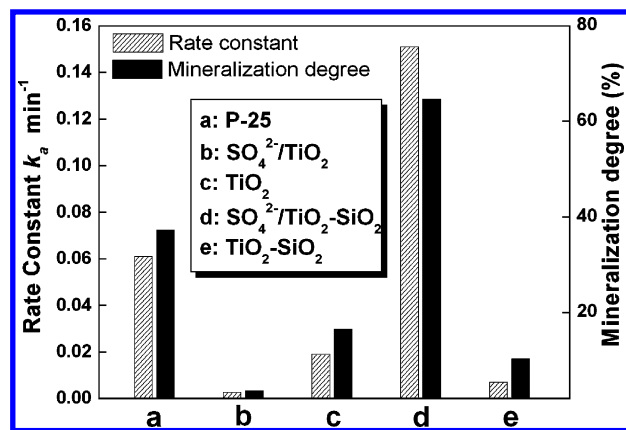


Figure 9. Rate constants and mineralization degrees of the catalysts for the gas-phase heterogeneous photodegradation of heptane.

covered by sulfate species. However, it is extremely strange that relatively well-crystallized anatase phase $\text{SO}_4^{2-}/\text{TiO}_2\text{-SiO}_2$ with a relatively lower sulfur content also does not show a SPS signal. In the previous literature²⁴ it has been proven that the mechanism of the SPS generation in nanosized semiconductor photocatalysts (TiO_2 and $\text{SO}_4^{2-}/\text{TiO}_2\text{-SiO}_2$ as well as P-25 in this study) is quite different from bulk semiconductor photocatalysts ($\text{SO}_4^{2-}/\text{TiO}_2$ and $\text{TiO}_2\text{-SiO}_2$ in this study). As far as crystallized nanoparticles are concerned, an intrinsic relationship between the intensity of SPS and the photocatalysis efficiency exists: the weaker the SPS signal, the higher the photocatalysis efficiency.²⁴ On the basis of Figure 8, the following order of photocatalysis efficiency for the crystallized nanosized photocatalysts in this study was constructed: $\text{SO}_4^{2-}/\text{TiO}_2\text{-SiO}_2 > \text{P-25} > \text{TiO}_2$. The absence of SPS signal for $\text{SO}_4^{2-}/\text{TiO}_2\text{-SiO}_2$, which is evidence for its highest photocatalysis efficiency among the three catalysts, can be explained by taking into account the presence of surface sulfate species and the new introduction of surface defects resulting from the formation of Ti–O–Si linkages, both of which can effectively capture photoinduced charge carriers. Moreover, the higher photocatalysis efficiency of P-25 than TiO_2 can be associated with its feature of coexistence of anatase and rutile phases, which has been proven to favor the separation of photoinduced electron–hole pairs.²⁵

3.5. Evaluation of the Photoactivities. The photoactivities of the catalysts were evaluated by gas-phase heterogeneous degradation of heptane under UV illumination. As shown in Figure 9, both $\text{SO}_4^{2-}/\text{TiO}_2$ and $\text{TiO}_2\text{-SiO}_2$ show very low photoactivity in that the surface of $\text{SO}_4^{2-}/\text{TiO}_2$ is predominantly covered by sulfate species and $\text{TiO}_2\text{-SiO}_2$ is amorphous, respectively. In the Introduction we said that either sulfation of titania or mixing titania with silica may be an effective approach to enhance the photocatalysis efficiency, which seems to be contrary to our experimental results. It has been widely accepted that preparation method, mainly involving the precursor and synthesis route used to synthesize photocatalysts, has a large influence on the surface properties and photoactivities of the resultant catalysts.⁶ Thus, we attribute this discrepancy to the fact that the preparation method we adopted (hydrolysis of $\text{Ti}(\text{SO}_4)_2$ in the absence or presence of silica) is dramatically different from the traditional methods for preparing sulfated titania and titania–silica mixed oxide.

For $\text{SO}_4^{2-}/\text{TiO}_2\text{-SiO}_2$ both the photoactivity and mineralization degree of heptane are significantly enhanced, even higher than that of P-25. In $\text{SO}_4^{2-}/\text{TiO}_2\text{-SiO}_2$, due to the favorable synergetic effects between sulfate species and silica, anatase-phase titania is obtained without forming the rutile phase upon 500 °C calcination, meaning bulk defects will be effectively

removed.²⁶ Furthermore, its smaller crystalline size (15.4 nm) is another important contribution to its excellent photoactivity. As widely recognized, the smaller crystalline size allows the faster arrival of photoinduced electron–hole pairs to surface, thus retarding the undesirable photocarrier recombination inside photocatalysts.²⁷ Note, TiO_2 has better crystallization than $\text{SO}_4^{2-}/\text{TiO}_2$ but shows obviously lower photoactivity. Ying et al. reported that anatase-phase titania with a crystalline size of about 10 nm is favorable for obtaining superior photocatalysis efficiency due to the low recombination rate of photoinduced electron–hole.²⁸ This demonstrates that crystalline size and structure property of nanoparticles are two important factors influencing the performance of photocatalysts. Obviously, the crystalline size of $\text{SO}_4^{2-}/\text{TiO}_2\text{-SiO}_2$ (15.4 nm) is very close to 10 nm, while that of TiO_2 (32.8 nm) exceeds that by much, which should be responsible for its inferior photoactivity.

According to XRD and FT-IR results, along with the theory proposed by Ward and Ko,⁷ we believe the surface sulfate species on $\text{SO}_4^{2-}/\text{TiO}_2$ are inactive (more ionic character and less inductive potential), which is detrimental to photocatalysis reactions because these inactive surface sulfate species occupy the photoactive sites and thereby lower the efficiency of titania utilizing the UV light energy. However, those on $\text{SO}_4^{2-}/\text{TiO}_2\text{-SiO}_2$ should be in the active form because $\text{SO}_4^{2-}/\text{TiO}_2\text{-SiO}_2$ possesses crystallized titania and exhibits excellent photoactivity.⁷ In addition, since the active and inactive surface sulfate species have distinct FT-IR fingerprints, the completely different FT-IR spectra of $\text{SO}_4^{2-}/\text{TiO}_2$ and $\text{SO}_4^{2-}/\text{TiO}_2\text{-SiO}_2$ should be strong evidence to support this conclusion. Thus, its enhanced photocatalysis efficiency should partially result from the active surface sulfate species. In the presence of active surface sulfate species, photoinduced electrons will be retained in their vicinity and photoinduced holes are concentrated in the body of titania. Thus, the undesirable recombination of photoinduced electron–hole pairs is effectively hindered to maintain the photoinduced charge carriers long enough to react with O_2 and H_2O to produce a series of extraordinarily reactive species capable of oxidizing the adsorbed substrates.²

4. Conclusions

Herein, we report a simple and efficient approach that can be applied to produce highly active nanocrystalline $\text{SO}_4^{2-}/\text{TiO}_2\text{-SiO}_2$ and reveal the favorable synergetic effects between sulfate species and silica in enhancing its photocatalysis efficiency. In the absence of silica, the surface of $\text{SO}_4^{2-}/\text{TiO}_2$ is dominantly covered by inactive surface sulfate species owing to the formation of inert titanyl sulfate. Without sulfate species $\text{TiO}_2\text{-SiO}_2$ is amorphous because of the excessive interaction between titania and silica, so that the crystallization of titania is prohibited. However, due to the favorable synergetic effects between sulfate species and silica, the physicochemical properties of $\text{SO}_4^{2-}/\text{TiO}_2\text{-SiO}_2$ are dramatically enhanced. First, silica is capable of promoting the decomposition of sulfate species resulting from the thermal instability of sulfate species on it, thereby avoiding formation of inert titanyl sulfate. Second, active sulfate species not only promote the separation of photoinduced electron–hole pairs due to their strong electron-withdrawing effect, but also exist between titania and silica as a protection layer to hinder their excessive interaction. Hence, $\text{SO}_4^{2-}/\text{TiO}_2\text{-SiO}_2$ possesses relatively well-crystallized and smaller-size anatase-phase titania without forming the rutile phase upon 500 °C calcination. Moreover, SPS results prove it possesses superior photocatalysis efficiency because of the active sulfate species

and the new introduction of surface defects due to the formation of Ti–O–Si linkages. According to the above facts it can be said that $\text{SO}_4^{2-}/\text{TiO}_2\text{--SiO}_2$ takes advantage of the positive effects of sulfate species and silica while effectively avoiding their negative effects on the physicochemical properties of titania. In summary, this study is the first to report that the greatly improved photoactivity performance of titania can be achieved through a simple and efficient approach, that is, simultaneous introduction of sulfate species and silica (hydrolysis of $\text{Ti}(\text{SO}_4)_2$ in the presence of silica), which can result in the synergetic effects that are favorable for enhancing the physicochemical properties.

Acknowledgment. This work was supported by a grant from the National Natural Science Foundation of China (20277015).

References and Notes

- (1) Hoffman, M. R.; Martin, S. T.; Choi, W. Y.; Bahnemann, D. W. *Chem. Rev.* **1995**, *95*, 69.
- (2) Linsebigler, A. L.; Lu, G.; Yates, J. T., Jr. *Chem. Rev.* **1995**, *95*, 735.
- (3) Mor, G. K.; Shankar, K.; Paulose, M.; Varghese, O. K.; Grimes, C. A. *Nano Lett.* **2005**, *5*, 191.
- (4) Yang, Q. J.; Xie, C.; Xu, Z. L.; Gao, Z. M.; Du, Y. G. *J. Phys. Chem. B* **2005**, *109*, 5554.
- (5) Jung, S. M.; Grange, P. *Appl. Catal. A* **2002**, *228*, 65.
- (6) Colon, G.; Hidalgo, M. C.; Navio, J. A. *Appl. Catal. B* **2003**, *45*, 39.
- (7) Ward, D. A.; Ko, E. I. *J. Catal.* **1994**, *150*, 18.
- (8) Hu, C.; Wang, Y. Z.; Tang, H. X. *Appl. Catal. B* **2001**, *30*, 277.
- (9) Xie, C.; Xu, Z. L.; Yang, Q. J.; Li, N.; Zhao, D. F.; Wang, D. B.; Du, Y. G. *J. Mol. Catal. A* **2004**, *217*, 193.
- (10) Yang, Q. J.; Xie, C.; Xu, Z. L.; Gao, Z. M.; Li, Z. H.; Wang, D. J.; Du, Y. G. *J. Mol. Catal. A* **2005**, *239*, 144.
- (11) Jung, K. Y.; Park, S. B. *Appl. Catal. B* **2000**, *25*, 249.
- (12) Li, Y. Z.; Kim, S. J. *J. Phys. Chem. B* **2005**, *109*, 12309.
- (13) Fu, X.; Clark, L. A.; Yang, Q.; Anderson, M. A. *Environ. Sci. Technol.* **1996**, *30*, 647.
- (14) Jung, S. M.; Dupont, O.; Grange, P. *Appl. Catal. A* **2001**, *208*, 393.
- (15) Lopez, T.; Bosch, P.; Tzompantzi, F.; Gomez, R.; Navarrete, J.; Lopez-Salinas, E.; Llanos, M. E. *Appl. Catal. A* **2000**, *197*, 107.
- (16) Parida, K. M.; Samantaray, S. K.; Mishra, H. K. *J. Colloid Interface Sci.* **1999**, *216*, 127.
- (17) Li, Z. H.; Wang, D. J.; Wang, P.; Lin, Y. H.; Zhang, Q. L.; Yang, M. *Chem. Phys. Lett.* **2005**, *411*, 511.
- (18) Yu, J. C.; Wang, X. C.; Fu, X. Z. *Chem. Mater.* **2004**, *16*, 1523.
- (19) Huang, Y. Y.; Zhao, B. Y.; Xie, Y. C. *Appl. Catal. A* **1998**, *171*, 65.
- (20) Xie, C.; Xu, Z. L.; Yang, Q. J.; Xue, B. Y.; Du, Y. G.; Zhang, J. H. *Mater. Sci. Eng. B* **2004**, *112*, 34.
- (21) Mishra, M. K.; Tyagi, B.; Jasra, R. V. *Ind. Eng. Chem. Res.* **2003**, *42*, 5727.
- (22) Mishra, M. K.; Tyagi, B.; Jasra, R. V. *J. Mol. Catal. A* **2004**, *223*, 61.
- (23) Stakheev, A. Y.; Shpiro, E. S.; Apijok, J. *J. Phys. Chem.* **1993**, *97*, 5668.
- (24) Jing, L. Q.; Sun, X. J.; Cai, W. M. *Sol. Energy Mater. Sol. Cells* **2003**, *79*, 133.
- (25) Sun, B.; Vorontsov, A. V.; Smirniotis, P. G. *Langmuir* **2003**, *19*, 3151.
- (26) Jung, K. Y.; Park, S. B. *J. Photochem. Photobiol. A* **1999**, *127*, 117.
- (27) Bickley, R. I.; Stone, F. S. *J. Catal.* **1973**, *31*, 389.
- (28) Zhang, Z. B.; Wang, C. C.; Zakaria, R.; Ying, J. Y. *J. Phys. Chem. B* **1998**, *102*, 10871.